Ab initio study of the stokes shift of the *n*s-*n*p transition of Tl^+ and In^+ in KCl, Jahn-Teller effect in the *nsn*p configuration

2001 J. Phys.: Condens. Matter 13 5597

(http://iopscience.iop.org/0953-8984/13/24/306)

INSTITUTE OF PHYSICS PUBLISHING JOURNAL OF PHYSICS: CONDENSED MATTER

J. Phys.: Condens. Matter **13** (2001) 5611–5624 www.iop.org/Journals/cm PII: S0953-8984(01)18283-4

Ab initio study of the stokes shift of the ns–np transition of Tl^+ and In^+ in KCl, Jahn–Teller effect in the $ns np$ configuration

J Andriessen, M Marsman and C W E van Eijk

Interfaculty Reactor Institute of the Delft University of Technology, Mekelweg 15, 2629 JB Delft, The Netherlands

Received 24 September 2000, in final form 8 March 2001

Abstract

Detailed lattice relaxation studies of the excited $ns np$ states of Tl^+ and In^+ in KCl have shown that the calculated Stokes shift of the 6s–6p transition of Tl^+ is most sensitive to the accuracy of the lattice relaxation around the substituted ion. This is a result of the strong cancellation between the influence of the spin–orbit interaction and the lattice relaxation on the 6s6p level positions. The results were calculated with a HF–LCAO embedded cluster method as well as with a DFT based supercell approach. Unexpectedly the supercell method completely fails for thallium in predicting the Stokes shift. Using the embedded cluster method, a value of 0.706 eV was found for the shift for thallium and 1.24 eV for indium. The experimental values are 0.88 and 1.44 eV respectively. It was also clearly established that the temperature dependence of the decay time of the main emission line of thallium is directly related to the Jahn–Teller distortion by which the trapping $^3A_{1u}$ level approaches the emitting $^3T_{1u}$ level. For indium this does not play a role because of the much smaller spin–orbit interaction.

1. Introduction

Recently the Stokes shift was studied for cerium in $LiBaF_3$ [1] and in $LaCl_3$ [2]. The remarkable fact was found that the local geometry of the relaxed excited state (5d for Ce^{3+}) was quite different from that of the ground state, showing a profound influence of excited states of ions on the local lattice structure. A second result of these studies was the extent of the relaxing region. If this is chosen too small there is almost no change in geometry and the Stokes shift comes out much too small.

In this work we address the more complicated ns^2–$ns np$ transition, on which a rich literature exists [3–5]. The complex absorption and emission spectra of these systems have been explained to a large extent, but mainly qualitatively. However a convincing explanation of the experimental results has never been given.

In this work the emphasis is on quantitative aspects of the physics of the main emission line of Tl^+ and In^+ in KCl.

0953-8984/01/245611+14$30.00

The $nsnp$ configuration for the free Tl^+ or In^+ ion has 12 states grouped into four levels. These levels are $^3P_0$, $^3P_1$, $^3P_2$ and $^1P_1$. The second and fourth are mixed by spin–orbit interaction. In the solid KCl (not distorted) the third level will split in two but this is almost never observed. The absorption lines are transitions to all levels except the first and are called A, B and C lines respectively. The single emission line observed comes from the $^3P_1$ level. In the solid this is the $^3T_{1u}$ level. We will maintain the nomenclature of the undistorted lattice also when the Jahn–Teller distortion breaks the symmetry.

Now the complication is that after absorption to the $^3T_{1u}$ state, the interaction with phonons will cause a non-radiative transition to the $^3A_{1u}$ ($^3P_0$) trapping level, which cannot decay to the ground state. In this state the system will relax to a local geometry of tetragonal symmetry by the Jahn–Teller effect. Because of this, the relaxed $^3T_{1u}$ state will become almost degenerate with the $^3A_{1u}$ state and the slow emission component arises from thermal excitation from $^3A_{1u}$ to $^3T_{1u}$.

There is also a small fraction of the dopant ions, which remain in the $^3T_{1u}$ state and the lattice will relax to a tetragonal distortion. This gives the fast component in the emission, which we do not consider here.

The actual distortion of the lattice was calculated from first principles and the Stokes shift was found from the energy changes of the relaxed excited $^3T_{1u}$ state and the $^1A_{1g}(6s^2)$ ground state. Additionally, the distance between the levels $^3A_{1u}$ and $^3T_{1u}$ in the distorted geometry will give an estimate of the temperature dependence of the transition time of the emission line using the exponential expression for the emission from a trap [6].

We have chosen thallium because the spin–orbit interaction in the 6s6p states is so large ($\lambda \sim 8000\,cm^{-1}$) that the lattice relaxation in the 6s6p states of interest is substantially reduced. This is because the lattice relaxation partially quenches the effect of the spin–orbit interaction. This interaction lowers the energy of the $^3A_{1u}$ and $^3T_{1u}$ states and so this lowering is reduced by relaxation.

It is also the most frequently investigated system with very detailed experimental data. With KCl as host, the emission characteristics are not too complicated and the relaxation model can be kept simple.

Indium is interesting because the relaxation is expected to be very similar to that of thallium but the Stokes shift is much larger. Furthermore the decay time of the emission line of indium in KCl shows hardly any temperature dependence. This different behaviour should be related to the much smaller spin–orbit interaction.

2. Theoretical models

The basic theoretical approach is essentially the same as that of our earlier work on $LiBaF_3$:Ce and $LaCl_3$:Ce. For the purpose of comparison two methods were used. The first is the widely used supercell approach, where in a cell of $3 \times 3 \times 3$ lattice units one potassium ion is replaced by the dopant ion. The electronic structure was calculated in the spin polarized DFT formalism.

The second method is an ionic cluster approach where the Tl^+ (or In^+) ion is part of a molecular fragment (cluster) of the lattice. The electronic structure of the ns^2 ground state and the triplet $nsnp$ excited state was calculated within the UHF–LCAO framework. The cluster has to be embedded in the crystal. For this we have used a sophisticated embedding procedure, in which the representation of the crystal outside the cluster can include both polarization and relaxation of the lattice ions. We will give more details further on.

The relaxation of the chosen structures is the key problem. For the supercell a molecular dynamics calculation is done where all ions in the supercell relax to equilibrium positions with a fixed size of the supercell. The main problem is the influence of the periodic boundary

conditions, which cancel all multipole moments of the supercell, and also restricts the relaxation of the outer region. Therefore the supercell should be as large as possible.

For the embedded cluster method we have relaxation of the cluster and of the embedding surroundings. Particularly the last part requires special attention. Details will be given below.

2.1. Spin–orbit interaction

The program packages we have used for the relaxation studies do not include spin–orbit interaction and so no spectroscopic levels are obtained. The levels arising from the $ns$$n$p configurations had to be calculated *a posteriori* using a parameter model. In order to check the limitations of this approach the unrelaxed geometry was also handled with a contemporary four-component Dirac–Fock quantum chemical cluster program, where the spin–orbit interaction is included in the (Dirac) Hamiltonian and the spectroscopy of the $ns$$n$p levels is well treated.

2.2. Program resources and theoretical formalism

The embedded cluster calculations were done with the DCLUSTER99 [7] program which is a combination of the classical GULP [8] code for the embedding procedure and the well known chemical code Gaussian 98 [9], which treats the cluster of ions quantum chemically. The interface was written by Sushkov *et al* [10].

The cluster of ions was chosen to consist of an $MCl_{12}K_{18}$ fragment. M is the dopant ion and it is surrounded by six nearest neighbour chlorine ions at half the lattice constant a_0 and 12 next nearest neighbour potassium ions at $0.5\sqrt{2}a_0$. Intentionally six potassium ions at a_0 and six chlorine ions at $1.5a_0$, all on the x, y and z axes, were added. This was done to obtain a more realistic relaxation in the triplet state, which is expected to give an elongation along the z axis and a contraction in the x and y directions because of the Jahn–Teller effect.

The embedding procedure models the environment of the cluster as a cubic nano-cluster, with a size of $13 \times 13 \times 13$ KCl unit cells consisting of polarizable point charges at the lattice sites, excluding those of the cluster of ions.

This nano-cluster is divided in two regions. The first region is spherical and has a radius of $2.87a_0$. Apart from the Coulomb interaction the charges in this region interact with each other and the ions of the cluster using a Buckingham potential for the repulsion between any atom pair:

$$V = A\exp(-r/r_0) - C/r^6 \tag{1}$$

where r is the distance between the atoms.

The shell parameters for simulating the polarization are the spring constant k in the expression $E = 0.5kx^2$ and the values of the core and the shell charges q_c and q_s, a distance x apart. These constants and those of the Buckingham potential were taken from [11] and are listed in table 1.

Table 1. Pair potential parameters and spring constants of the lattice shell model for pure KCl [11].

Ion1	Ion2	A (eV)	r_0 (Å)	C (eV Å^{-6})	k (eV Å^{-2})	q_c	q_s
K	K	6.172×10^9	0.1085	36.22	484.82	6.96	−5.96
Cl	Cl	3361.0	0.3564	193.92	31.33	1.653	−2.653
K	Cl	4853.0	0.3080	80.64			

The total energy of the ionic cluster and the charges of region I is minimized with respect to the electronic and positional parameters of the ionic cluster and the charges.

The second region consists of all point charges outside the first region. Here the point charges are fixed and can not polarize. They serve to approximate the potential of the infinite crystal up to a constant. Further details about the approach can be found in [7] and [8].

In the HF–LCAO cluster calculation we have used the following Gaussian basis sets. For thallium and indium 21 electron relativistic ECP bases [12] were taken. For chlorine a seven electron ECP basis was used, the CEP-121G of the g98 package and an all electron 4333/43 basis was chosen for potassium.

The 21 electron bases for thallium and indium proved to be the best choice compared to earlier used 13 electron bases. The larger flexibility of these bases causes a larger inward movement of four of the six nearest neighbour chlorine ions on relaxation and so the Stokes shift increases.

The ns^2 ground state of the dopant ion is found from a ground state calculation of the cluster fragment.

To obtain the right relaxation in the triplet state it is mandatory to start already with a slight elongation along the z axis, because otherwise no pure occupation of the np_z orbital is realized.

For the supercell calculation use has been made of the package VASP [13]. We have used the ultrasoft pseudo-potentials of Kresse and Haffner [14] supplied with the program. Exchange and correlation were treated in the generalized gradient approximation (GGA), based on the parametrization by Perdew and Zunger [15] of the local-density functional of Ceperley and Alder [16] with the gradient corrections following Perdew and Wang [17] (PW91).

We had a [Kr] core for indium, a [Xe]$4f^{14}$ core for thallium, both with a $d^{10}s^2p^1$ valence configuration, a [Ne] core for chlorine with a $3s^23p^5$ valence shell and a [Mg] core for potassium with a $3p^64s$ electron configuration.

The kinetic energy cutoff was chosen to be 219.5 eV for the plane-wave representation of the wavefunctions and 600.0 eV for the augmentation charge density. Because of the very time consuming calculations the supercell was chosen to be a block of $3 \times 3 \times 3$ unit cells and only one k-point was taken, the gamma point. The calculations were done for up-spin as well as down-spin orbitals.

The calculations for the ns^2 ground state are straightforward, but those of the excited triplet state are more elaborate. We had to excite a down-spin electron in the 5s (6s) band to the lowest up-spin 5p (6p) band. This is usually not easy with a band structure calculation. However because of the localized nature of the bands of interest and the fact that only one k-point was taken, this could be accomplished using standard options in the program. Again the relaxation was started with a small elongation in the z direction, because otherwise the correct np orbital would not be occupied.

Next, details are given about the parameter model for including spin–orbit interaction and modelling the Jahn–Teller coupling.

2.3. Model for the nsnp configuration interacting with the lattice

Several authors have published the solution of the Hamiltonian equation of the 12 states of the $nsnp$ configuration interacting with the lattice. We will use equations of [4], somewhat extended to serve our purpose.

The key Hamiltonian is written as follows.

$$H = H_0 + H_{ls} + H_{elast} + H_{jt} \tag{2}$$

$$H_0 = -\hbar^2/2m\nabla^2 + V(r) \tag{3}$$

$$H_{ls} = \lambda(\boldsymbol{l}_1 \cdot \boldsymbol{s}_1 + \boldsymbol{l}_2 \cdot \boldsymbol{s}_2) \tag{4}$$

$$H_{elast} = 0.5K_\varepsilon(Q_3^2 + Q_2^2) \tag{5}$$

$$H_{jt} = b(Q_2 + Q_3/\sqrt{3}). \tag{6}$$

H_0 is the one-electron model Hamiltonian of the lattice relaxation model mentioned above, i.e. Hartree–Fock in case of the cluster calculations and DFT for the supercell band structure approach.

The spin–orbit term H_{ls} shows the spin–orbit interaction of the ns and the np electron. The elastic Hamiltonian H_{elast} contains the operators Q_2 and Q_3, which work on the x, y and z components of the orbital triplet terms of the nsnp configuration. The eigenvalues are expressed in terms of the distortion coordinates q_2 and q_3 [18] of the Cl_6 fragment around the dopant ion. If we denote the displacements of the three chlorine neighbours on the positive axes by dx, dy and dz, we have $q_2 = dx - dy$ and $q_3 = 1/\sqrt{3}(2dz - (dx + dy))$. The notation is such that for q_2, dy has to be $-dx$ and for q_3 both dx and dy have to be equal to $-\frac{1}{2}dz$. In this way the volume is kept constant. The displacement of the ions on the negative axes is included in this notation [18]. The parameter K_ε will be a result of our relaxation study.

The Jahn–Teller Hamiltonian H_{jt} describes the first order coupling of the np orbitals with the distortion coordinates q_2 and q_3. The constant b is the coupling parameter we will determine from our calculations.

The three orbital and four spin combinations of the nsnp configurations can be combined in 12 basis functions in terms of which the Hamilton matrix blocks out into four 3×3 matrices.

It is quite common to transform to a dimensionless form by introducing the variables $x_{2,3} = -b/(2\sqrt{3}\lambda)q_{2,3}$, $A = 6\lambda K_\varepsilon/b^2$ and $g = G/\lambda$.

G is half the triplet–singlet splitting with neglect of spin–orbit interaction.

There are essentially three matrices which describe the properties of the levels as a function of the parameters A, λ and G. The first one, shown in equation (7), gives the position of the singlet $^3A_{1u}$ ($^3P_0$) and the doublet ^3E_u ($^3P_2$) levels. We have simplified the expression by setting $x_2 = 0$, because there is good evidence thallium and indium in KCl show only tetragonal distortions and so x_2 is not required.

$$H_1 = E_0 I + \lambda \begin{pmatrix} Ax_3^2 + 2x_3 & -0.5 & -0.5 \\ -0.5 & Ax_3^2 + 2x_3 & -0.5 \\ -0.5 & -0.5 & Ax_3^2 - 4x_3 \end{pmatrix}. \tag{7}$$

E_0 is the energy of the triplet state without spin–orbit interaction and without distortion ($x_3 = 0$). This parameter follows from the relaxation studies but is not used further.

There are minima for positive and negative x_3. For our case the one for positive x_3 is most pronounced and gives the $^3A_{1u}$ level. If x_2 is included other minima exist, with the tetragonal distortion directed along the other axes. A peculiar aspect of (7) is the counterbalance between the effect of spin–orbit interaction represented by the numbers 0.5 and the relaxation term with the x_3 parameter. Actually the larger x_3 the smaller is the effect of the spin–orbit interaction because of the increasing distance to the $^3E_{1u}$ level.

The second and third matrices, shown in equations (8) and (9), give the behaviour of the $^3T_{1u}$ ($^3P_1$), $^3T_{2u}$ ($^3P_2$) and the $^1T_{1u}$ ($^1P_1$) levels. If we include the x_2 coordinate the two equations are equivalent.

$$H_2 = E_0 I + \lambda \begin{pmatrix} Ax_3^2 + 2x_3 & 0.5 & -0.5\mathrm{i} \\ 0.5 & Ax_3^2 + 2x_3 & 0.5\mathrm{i} \\ 0.5\mathrm{i} & -0.5\mathrm{i} & Ax_3^2 - 4x_3 + 2g \end{pmatrix} \tag{8}$$

$$H_3 = E_0 I + \lambda \begin{pmatrix} Ax_3^2 + 2x_3 & 0.5 & -0.5\mathrm{i} \\ 0.5 & Ax_3^2 - 4x_3 & 0.5\mathrm{i} \\ 0.5\mathrm{i} & -0.5\mathrm{i} & Ax_3^2 + 2x_3 + 2g \end{pmatrix}. \tag{9}$$

The most important feature of these equations is that there is a deep minimum of the $^3T_{1u}$ state for positive x_3 (equation (9)), more or less at the same value as for the $^3A_{1u}$ level of equation (7). The $^3T_{1u}$ state is the emitting and $^3A_{1u}$ the trapping level in the physics of the emission.

The equations given above are very helpful for analysing the emission spectrum. However the mixing of the dopant orbitals with the ligands is neglected. It is assumed that the parameters G and λ can take this into account if we extract these from the absorption lines. In the following section one can see that this leads to a value of G which is much smaller than that of the free ion and also λ is reduced.

Because in our relaxation study λ is zero, the behaviour of the minimum of the $^3T_{1u}$ state is simple and we can derive the following equations for the variables b and K_ε expressed in terms of the resulting relaxation.

If the lowering of the triplet state by relaxation from the unrelaxed (ns^2) geometry to the relaxed geometry is E_{relax} and the corresponding lattice distortion is q_3 we have

$$b = \sqrt{3}E_{relax}/q_3 \tag{10}$$

$$K_\varepsilon = -2E_{relax}/q_3^2. \tag{11}$$

The usefulness of the quadratic expression of the relaxation with a single distortion coordinate was thoroughly tested. Actually there is a contribution of the breathing mode coordinate q_1, but the influence was found to be negligible.

3. Results

3.1. Ab initio energy levels of Tl^+ in KCl

In order to perform a test on the usefulness of the model explained above for a heavy ion like thallium we give results of a comparison of *ab initio* energy levels of Tl^+ in KCl in the undistorted geometry with those of the absorption experiments. The method we have used is the fully relativistic Dirac–Fock LCAO method implemented in the code MOLFDIR [19]. The spin–orbit interaction is now included in the right way. Limited configuration interaction (cosci) was done on the 6s6p configuration. Unfortunately no relaxation can be studied with this code.

In table 2 the results are listed of energy levels of Tl^+ calculated with the Dirac–Fock code and with the parameter model described above. The parameters λ, G and E_0 were obtained from the second, third and fourth 6s6p energy level. These parameters are not enough for matching all levels. The mismatch for the first level ($^3A_{1u}$) in the table gives an indication of the model error. It is a result of relativistic effects which result in two 6p orbitals, one for $6p_{1/2}$ and one for $6p_{3/2}$, and this is not accounted for in the parameter model.

For a reasonable fit to the experimental values, particularly the value of G has to be readjusted to a much smaller value. This is due to charge transfer from the chlorine ions to the empty 6s levels. This decreases the triplet-singlet splitting considerably. The final values $G = 0.28$ eV and $\lambda = 0.69$ eV are in reasonable agreement with the values given in [5]. The spin–orbit parameter is found to be only slightly smaller than that from the Dirac–Fock calculation.

The MOLFDIR calculation does not include correlation effects and so the charge transfer mentioned above is not large enough. The interaction with the conduction band levels, included in a CI calculation, is assumed to bridge the gap. No attempt was done to do this, because our main issue is the behaviour of the triplet levels and the influence of lattice relaxation.

Table 2. Comparison of *ab initio* energy levels of Tl^+ in KCl, obtained with the MOLFDIR code, with results of the parameter model and with experiment. The notation A, B and C refers to the nomenclature of the absorption lines. All values are in eV.

	MOLFDIR levels	Parameter model	
		Model levels	Fit to experiment
Parameters			
E_0	—	5.30	5.58
λ	—	0.78	0.69
G	—	1.03	0.28
Levels			
6s	0	0	0
6s6p			
$^3A_{1u}$	4.43	4.52	—
$^3T_{1u}$ (A)	4.79	4.79	5.03
$^3T_{2u}$, ^3E_u (B)	5.69	5.69	5.93
$^1T_{1u}$ (C)	7.48	7.48	6.36

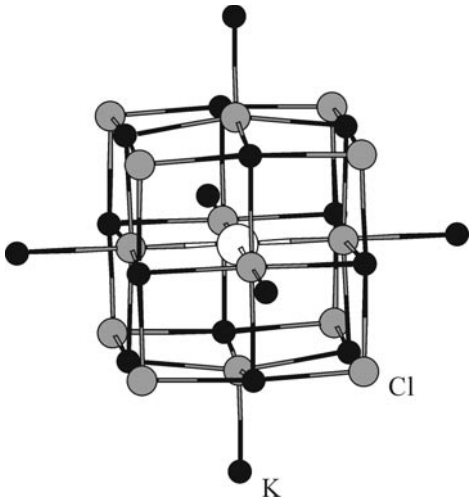

Figure 1. Jahn–Teller distortion of the local environment of a Tl^+ or In^+ dopant excited to the nsnp configuration. Up to the fourth neighbour ring is shown. The relaxation shows the actual distortion for the In^+ defect.

3.2. Lattice relaxation studies of the nsnp levels of Tl^+ and In^+ in KCl

3.2.1. Supercell approach. There are two types of relaxation. The first one is for the ns^2 ground state with only radial relaxation. The symmetry remains cubic. The second one, for the nsnp state, is shown in figure 1, where the neighbours up the fourth shell are indicated. There is an elongation in the z direction and a contraction in the x and y directions. The occupied np orbital has to be the np_z orbital. This last point is crucial. With a band structure approach like that used in VASP this is not a simple matter in general because of the Bloch-type wavefunctions. By taking only the gamma point in the first Brillouin zone, the particular band can be occupied by applying already at the start of the relaxation a slight tetragonal distortion. After inspecting the character of the bands the right occupation could be obtained.

The supercell was chosen in two ways. First a $2 \times 2 \times 2$ unit block with 64 ions was taken, so that the neighbours up to the third shell were able to relax to a certain extent, but actually it is a direct neighbour relaxation. A much more realistic supercell is the $3 \times 3 \times 3$ block with 216 ions, because now the potassium neighbours on the x, y and z axes, which feel directly the

Table 3. Results of lattice relaxation around a Tl^+ centre in KCl calculated with the supercell approach. Thallium is in the 6s6p triplet state. Positions are given in terms of the lattice constant, which was found from the optimized geometry to be 6.3137 Å. Up to the fifth neighbour shell is shown. The supercell was a $3 \times 3 \times 3$ unit. The numbers in bold case are those with the largest relaxation. The start positions are those of the relaxed geometry for the ground $6s^2$ state.

Ion	Shell	x, y, z start positions ($6s^2$ end positions)			x, y, z end positions		
Cl	1	0.505 57	0.0	0.0	**0.472 79**	0.0	0.0
		0.0	0.0	0.505 57	0.0	0.0	**0.56 324**
	3	0.499 74	0.499 74	0.499 74	0.500 89	0.500 89	0.497 69
	5	0.0	0.499 92	1.000 12	0.0	0.503 85	1.004 33
		1.000 12	0.499 92	0.0	0.995 60	0.496 65	0.0
		1.000 12	0.0	0.499 92	0.998 83	0.0	0.497 55
K	2	0.499 82	0.499 82	0.0	0.500 45	0.500 45	0.0
		0.499 82	0.0	0.499 82	**0.487 61**	0.0	0.503 46
	4	1.00021	0.0	0.0	0.99821	0.0	0.0
		0.0	0.0	1.000 21	0.0	0.0	**1.026 92**

Table 4. Energy level parameters of Tl^+ and In^+ in KCl using the supercell approach.

Dopant	E_0 (eV)	E_{relax} (eV)	q_3 (Å)	b (eV Å^{-1})	K_ε (eV Å^{-2})	K_{ns} (eV Å^{-2})
Tl	4.90	−0.296	0.659	−0.778	1.36	1.81
In	4.09	−0.408	0.699	−1.01	1.67	1.97

movement of the six nearest neighbours, are able to relax. For the latter supercell the direct relaxation results for thallium in the 6s6p triplet state are given in table 3. We have reduced the information as much as possible, taking into account the tetragonal D_{4h} symmetry. Up to the fifth neighbour shell is documented. The lattice constant was found from the optimized geometry of pure KCl. The value 6.3137 Å is very near the value 6.2916 Å found from x-ray analysis. The energy change of the supercell by relaxation was found to be −0.296 eV. For the $2 \times 2 \times 2$ cell a value of −0.231 eV was calculated. The corresponding q_3 values were 0.659 and 0.461 Å respectively.

The data for indium are similar; the relaxation however is somewhat larger.

The results for the different parameters required for calculating the energy levels are tabulated in table 4. The E_0 parameter directly results from the energy difference between the $ns np$ state and the ns^2 state in the ns^2 optimized geometry. E_{relax} and q_3 result from the relaxation study and then b and K are calculated using equations (10) and (11).

The variable K_{ns} parametrizes the energy dependence of the ground state energy on the distortion coordinate q_3 in the form $E = 0.5 K_{ns} q_3^2$.

3.2.2. Embedded cluster approach. As was mentioned in the foregoing section the main cluster of ions consisted of the dopant ion, its six nearest and 12 next nearest neighbours. Considering the way of relaxation which is dominated by displacements of the ions on the x, y and z axes, the six potassium ions at one lattice unit (a_0) and the six chlorine ions at one and a half lattice units were added. The rest of the lattice in a block of $13 \times 13 \times 13$ lattice units was represented by point charges. The charges interact with the cluster and each other using a Buckingham potential of which those in a sphere of 2.87 a_0 can relax and polarize.

Different basis sets were employed and those with the largest relaxation were chosen. It

Table 5. Results of lattice relaxation around a Tl^+ centre in KCl calculated with the embedded cluster approach. Thallium is in the 6s6p triplet state. Positions are given in terms of the lattice constant, which was found from the optimized geometry to be 6.2422 Å. Up to the fifth neighbour shell is shown. The seventh shell is shown also because of the unexpected large relaxation of the chlorine ions on the axes. The relaxing region was a sphere with a radius of 2.87 lattice unit. The numbers in bold case have the largest relaxation. The start positions are those of the relaxed geometry for the ground $6s^2$ state.

Ion	Shell	x, y, z start positions ($6s^2$ end positions)			x, y, z end positions		
Cl	1	0.523 42	0.0	0.0	**0.480 17**	0.0	0.0
		0.0	0.0	0.523 42	0.0	0.0	**0.584 38**
	3	0.502 40	0.502 40	0.502 40	0.503 29	0.503 29	0.500 72
	5	0.0	0.502 09	1.0101	0.0	0.506 42	1.019 44
		1.0101	0.502 09	0.0	1.006 80	0.498 92	0.0
		1.0101	0.0	0.502 09	**1.000 04**	0.0	0.498 75
K	2	0.514 01	0.514 01	0.0	0.513 03	0.513 03	0.0
		0.514 01	0.0	0.514 01	**0.499 85**	0.0	**0.520 88**
	4	1.017 22	0.0	0.0	**1.0**	0.0	0.0
		0.0	0.0	1.017 22	0.0	0.0	**1.052 56**
C_t	7	0.0	0.0	1.521 67	0.0	0.0	**1.540 74**
		1.521 67	0.0	0.0	**1.513 06**	0.0	0.0
		1.000 69	1.000 69	0.500 01	1.000 90	1.000 90	0.499 335
		0.500 01	1.000 69	1.000 69	0.500 18	1.001 02	1.000 88

Table 6. Energy level parameters of Tl^+ and In^+ in KCl using the embedded cluster approach.

Ion	E_0 (eV)	E_{relax} (eV)	q_3 (Å)	b (eV Å^{-1})	K_ε (eV Å^{-2})	K_{ns} (eV Å^{-2})
Tl	5.19	−0.603	0.751	−1.39	2.14	2.39
In	3.74	−0.676	0.841	−1.39	1.91	2.03

appeared that the effective core of the dopant ion should be as small as possible and so we have chosen a 21 valence electrons flexible ECP basis, as was mentioned above. Also d-type polarization functions on the chlorine ions were added.

In table 5 the results are given of typical relaxations in the nsnp state. Table 6 lists the parameters obtained from these studies. Important in a comparison with the results of the supercell approach is that different levels of relaxation were used. It would take us too long if this were also documented. An important conclusion was that the relaxation of the ions outside the ones shown in table 5 contributed around 0.05 eV. So this is rather small. The relaxation of just the nearest neighbours gives only half the value of table 5. As was mentioned already, the relaxation is very much dominated by the displacements of the ions on the x, y and z axes. Note the fact that the chlorines in the seventh shell at 1.5 a_0 move around 0.2 Å which is still comparable with the displacement of the potassium ions at a_0.

It is evident that the relaxation obtained with the supercell method is comparable with that of the cluster method only with respect to the geometry. The energy gain E_{relax} (see tables 4 and 6) is however very different, particularly for thallium, where we find a factor of two disagreement.

There are two reasons for this. The first one is the effect of the periodic boundary conditions, which limits the displacement of the ions at larger distance. It is not practical to choose a much larger supercell than the one we have taken.

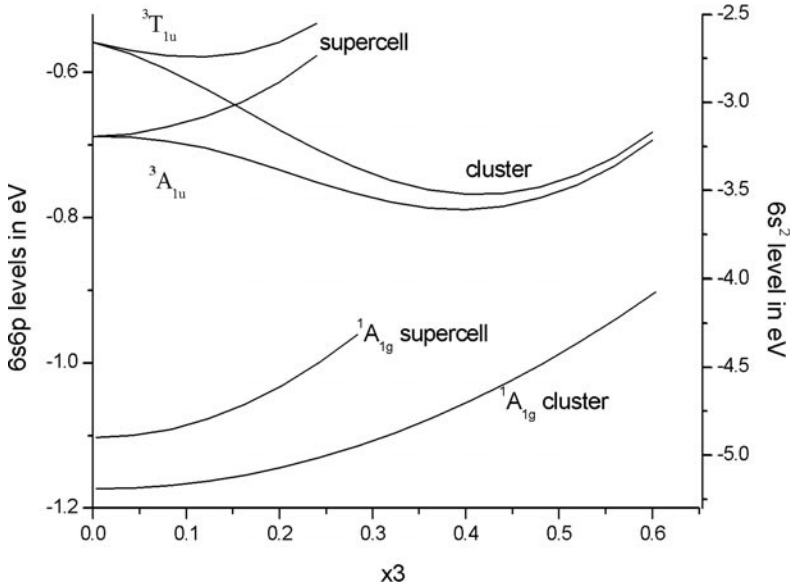

Figure 2. $6s^2$ and 6s6p triplet levels for thallium as a function of the tetragonal x_3 distortion coordinate. A double y axis is used for viewing the curves with equal precision. Results are given for the supercell approach using the VASP code and the cluster model with the Dcluster99 program. Absorption is supposed to occur at $x_3 = 0$ from $^1A_{1g}(6s^2)$ to $^3T_{1u}$ (6s6p). Subsequently this level depopulates to $^3A_{1u}$ by phonons. In this state the system relaxes to the minimum and emission by thermal excitation takes the system back to $^1A_{1g}$. On can see that this does not happen for the supercell calculation.

Another more important reason is the pseudo-potential used in the approach. The DFT form of the potentials and the fact that we have only a 13-electron basis for the dopant ion, are assumed to be the main reasons for the disagreement. Particularly the thallium potential seems to be too soft.

An estimate of the effect of including the inner 5s5p shells in the pseudo-potential core is around 0.1 eV and the effect of the boundary conditions is roughly 0.05 eV, as was mentioned earlier. The resulting 0.15 eV partially bridges the gap between the results of the two approaches. The mismatch of around 0.15 eV is very likely a limitation of the form of the ultrasoft pseudo-potential.

3.2.3. Level positions. We will now investigate the positions of the lowest levels of the dopant ion as a function of the x_3 coordinate using the model presented in section 2. In this way we can estimate the emission behaviour of the centre. The Stokes shift and the position of the trapping $^3A_{1u}$ level with regards to the emitting $^3T_{1u}$ level are the interesting quantities.

It is straightforward to obtain the curves of level position versus the x_3 coordinate for the thallium and indium centre using equations (7), (8) and (9).

This is done for the supercell as well as the cluster method. Comparing results of the two approaches best shows the delicate balance between energy gain by lattice relaxation and energy loss by the quenching of the spin–orbit interaction as was explained above in relation to equation (7). In figure 2 the results are shown of the thallium ion and in figure 3 those of the indium ion.

For thallium one can see that for the supercell approach there is no Jahn–Teller distortion at all, because the trapping level goes up as a function of the x_3 coordinate. There is a small

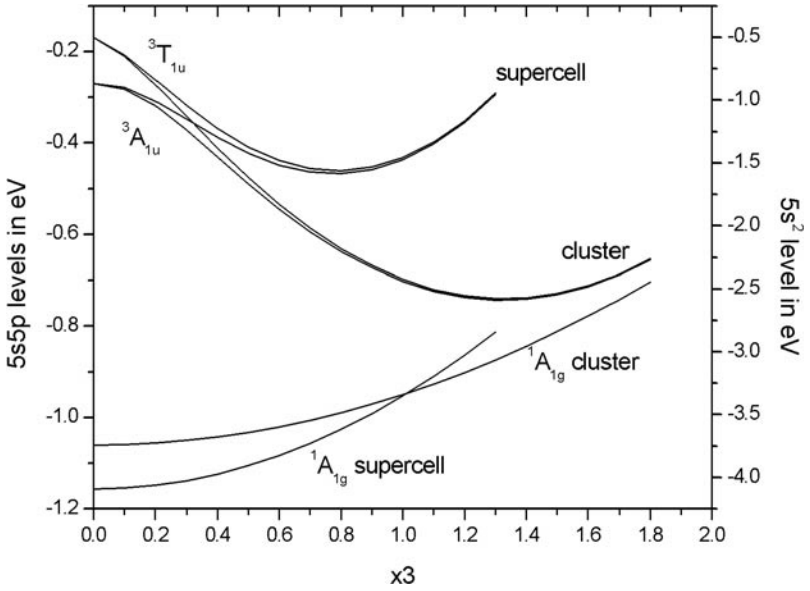

Figure 3. $5s^2$ and 5s5p triplet levels as a function of the tetragonal x_3 distortion coordinate. A double y axis is used for viewing both curves with equal precision. Results are given for the supercell approach using the VASP code and the cluster model with the dcluster99 program. Absorption is supposed to occur at $x_3 = 0$ from $^1A_{1g}(5s^2)$ to $^3T_{1u}(5s5p)$. Subsequently this level depopulates to $^3A_{1u}$ by phonons. In this state the system relaxes to the minimum and emission by thermal excitation takes the system back to $^1A_{1g}$.

minimum in the $^3T_{1u}$ 6s6p level curve but the population would be much too small. The Stokes shift would be of the order of 0.1 eV.

The cluster results however show a pronounced minimum in the $^3A_{1u}$ curve. We see clearly the role of the trapping level $^3A_{1u}$. At zero distortion the distance to the $^3T_{1u}$ level is much too large to explain the measured decay time dependence on temperature. However as the distortion increases the two levels approach each other and at the minimum the energy difference is around 0.02 eV, which is comparable with the value of 0.05 eV found from experiment [20, 21]. We mentioned above that the parameter model underestimates the energy difference between these two levels (see table 2) and so this may explain the disagreement.

The Stokes shift was calculated from the minimum in the $^3T_{1u}$ curve and the corresponding energy change in the 6s curve (0.496 eV). The value of 0.706 eV compares reasonably well with the value of 0.88 eV found experimentally [22].

Now we turn to the indium case shown in figure 3. In this case the supercell as well as the cluster model show clear minima of the $^3A_{1u}$ and $^3T_{1u}$ curves. The only difference is the depth and position in x_3 space of the minima. For the supercell the Stokes shift amounts to 0.765 eV and for the cluster calculation one obtains 1.247 eV. The experimental value is 1.44 eV [23].

Again the cluster result is around 20% smaller than the experimental value. The fact that here also the supercell approach gives a Jahn–Teller distortion is because there is hardly any competition between the spin–orbit interaction and the lattice relaxation. This is because the spin–orbit interaction it is less than half that [5] in the thallium case. Another important feature of figure 3 is the extremely small energy difference between the $^3A_{1u}$ and $^3T_{1u}$ curves in the neighbourhood of the minima. Because of this there would be no temperature dependence of the decay time of the emission line, in agreement with experiment.

Table 7. Comparison of results of the embedded cluster calculation for the Stokes shift and intrinsic decay time of the emission lines of Tl^+ and In^+ in KCl. Also the position of the trapping level $^3A_{1u}$ with regard to the $^3T_{1u}$ level is tabulated.

	Stokes shift (eV)		Intrinsic decay time (μs)		Trap depth (eV)	
Ion	Calc.	Exp.	Calc.	Exp.	Calc.	Exp.
Tl	0.706	0.88[a]	0.09	0.1[b]	−0.021	−0.05[b]
In	1.247	1.44[c]	2.9	3[d]	0.0003	—

[a] [22] for the emission line. The absorption line (A) is found from table 2.
[b] [23] for the emission and [5] for absorption.
[c] [21].
[d] [3].

3.2.4. Decay time. It is interesting to calculate the decay time of the $^3T_{1u}$ level to the ground $^1A_{1g}$ ($6s^2$) level from values for the mixing coefficients of the $^1T_{1u}$ state in $^3T_{1u}$ and compare these with experiment. These are the so-called intrinsic decay times. The mixing depends on the Jahn–Teller distortion because of the shifting of levels. Only the cluster results are considered here.

We have used the following equation for the evaluation of the decay time [24].

$$A = 4n(n+2)^2 e^2 \omega^3 / (27\hbar c^3) \langle ns|z|np_z\rangle^2 \alpha_s^2. \tag{12}$$

A is the transition probability per second, n the refractive index ($n = 1.5$), ω is the frequency of the transition and α_s as the triplet-singlet mixing coefficient. The dipole element $\langle ns|z|np_z\rangle$ has the value 1.32 Å for thallium and 1.39 Å for indium, evaluated for the free ion. The mixing coefficient was found to be 0.167 for thallium and 0.048 for indium.

Table 7 gives an overview of our results on the Stokes shift and intrinsic decay times of the np–ns transition of thallium and indium in KCl compared with experiment.

4. Discussion and conclusions

The heavy thallium ion with the strong spin–orbit interaction has been found to be a critical case for lattice relaxation studies. Generally speaking lattice relaxation suffers from a lack of accurate experimental data to support the approach taken. In our case we have the effect of spin–orbit coupling which restrains the lattice relaxation of the Jahn–Teller effect. For the widely used approach of the supercell model in the DFT formulation of electron interaction the lattice relaxation is only half the size needed to balance the quenching of the spin–orbit interaction. Curiously enough the relaxation itself, i.e. the displacement, is of the right magnitude.

The fact that an excited state is considered, which is found to be in the conduction band of the KCl crystal, appears to be not directly responsible. This is because it was found that there is no mixing between the levels of interest and the nearest conduction band levels, a result of taking only the gamma point in k-space. In our opinion the pseudo-potentials are responsible for the mismatch.

The embedded cluster method in the HF–LCAO formulation of electron interaction is much more successful. However a lot of effort had to be spent in optimizing the basis set for obtaining the nice results we have presented above. It appears that for thallium the best model is an all electron model of the dopant ion in Dirac–Fock formulation of electron interactions. The parameter model explained above is very useful but limitations were found in the prediction of the level positions, in particular the $^3A_{1u}$ level.

The main profit of the embedded cluster model is the fact that we can put to relaxation thousands of ions, a task which is prohibitively time consuming in a pure HF–LCAO treatment of a part of the crystal large enough for obtaining a realistic relaxation. However most of the relaxing ions are classical point charge ions and so the wavefunctions in this part of the crystal are useless, but very likely this is not serious.

We have found that the usual practice of relaxing only the direct neighbours only amounts to half the final result. The relaxation region has to contain at least the fourth neighbour shells and has to feel the right repulsive forces with the fixed region. In our calculation we have chosen the relaxing region much larger, but this adds only some 10% to the final relaxation energy. The role of polarization in the embedding part was found to be almost negligible. However is has been found that it is important to add polarization functions of d-type to the basis set of the chlorine neighbours in the quantum chemical cluster part of the calculation. The results obtained for the Stokes shift and lifetimes and the support for the trapping model for the thallium dopant in KCl are very encouraging.

Our calculation and nice agreement of the decay times is partly fortuitous because the curves published in the literature do not always agree and the extraction of the decay times and excitation energy from the curves is not very accurate. But anyhow the agreement appears to prove the correctness of the model. Our model is completely different from that published in [25]. The authors do not use the trapping mechanism in explaining the decay times. The information given seems to point out that a semi-empirical method is used and so a comparison can not be made.

Many more experimental data are available for similar but more complicated cases. For instance indium in bcc KCl has two emission lines instead of the one we have treated here. Also thallium in KBr and KI shows two lines. Even more peculiar, thallium in CsI even shows three lines [26] if the system is put under pressure. The occurrence of these extra lines is tentatively explained by assuming the contribution of other minima in space of the normal coordinates. Also, very likely, in some cases higher order Jahn–Teller effects with additional coordinates contribute.

Our efforts will continue in the field of this more difficult part of the coupling of the dopant ion electrons to the lattice.

References

[1] Marsman M, Andriessen J and van Eijk C W E 2000 *Phys. Rev.* B **24** 16 477
[2] Andriessen J, Antonyak O T, Dorenbos P, Rodnyi P A, Stryganyuak G B, van Eijk C W E and Voloshinovskii A S 2000 *Opt. Commun.* **178** 355
[3] Fukuda A 1970 *Phys. Rev.* B **1** 4161
[4] Ranfagni A, Mugnai D, Bacci M, Viliani G and Fontana M P 1983 *Adv. Phys.* **32** 823
[5] Jacobs P W M 1991 *J. Phys. Chem. Solids* **52** 35
[6] Tomura M, Masuoka T and Nishimura H 1964 *J. Phys. Soc. Japan* **19** 1982
[7] Sushkov P V 1999 *Dcluster99* program University College London
[8] Gale J D 1997 *J. Chem. Soc. Faraday Trans.* **93** 629
[9] Frisch M J *et al* 1998 *Gaussian 98* revision A.1 (Pittsburgh PA: Gaussian)
[10] Sushkov P V, Schluger A L and Catlow C R A 2000 *Surf. Sci.* **450** 153
[11] Sangster M J L and Atwood R M 1978 *J. Phys. C: Solid State Phys.* **11** 1541
[12] Stevens W J, Krauss M, Basch H and Jasien P G 1992 *Can. J. Chem.* **70** 612
[13] Kresse G and Furthmüller J 1998 VASP 4.4.2 Technical University Vienna
[14] Kresse G and Hafner J 1994 *J. Phys.: Condens. Matter* **6** 8245
[15] Perdew J P and Zunger A 1981 *Phys. Rev.* B **23** 5048
[16] Ceperley D M and Alder B J 1980 *Phys. Rev. Lett.* **45** 566
[17] Perdew J P and Wang Y 1992 *Phys. Rev.* B **45** 13 244
[18] Öpik U and Pryce M H L 1957 *Proc. R. Soc.* **238** 425

[19] Visscher L, Visser O, Aerts P J C, Merenga H and Nieuwpoort W C 1994 *Comput. Phys. Commun.* **81** 120
[20] Illingworth 1964 *Phys. Rev.* **136** A508
[21] Tomura M and Nishimura H 1965 *J. Phys. Soc. Japan* **20** 1536. The actual parameters were found by fitting the published curve of decay time versus temperature with an exponential of the form $\tau^{-1}\exp(-e/kT)/(1+\exp(-e/kT)$.
[22] Donahue J M and Teegarden K 1968 *J. Phys. Chem. Solids* **29** 2141
[23] Drotning W D and Drickamer H G 1975 *Phys. Rev.* B **13** 4576
[24] Henderson B and Imbusch G F 1989 *Optical Spectroscopy of Inorganic Solids* (Oxford: Clarendon) p 160
[25] Rivas-Silva J F and Berrondo M 1996 *J. Phys. Chem. Solids* **57** 1705
[26] Klick D and Drickamer H G 1978 *Phys. Rev.* B **17** 952